

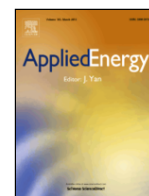


ELSEVIER

Contents lists available at ScienceDirect

Applied Energy

journal homepage: www.elsevier.com



Experimental evaluation of a semi-open membrane-based absorption heat pump system utilizing ionic liquids[☆]

Devesh Chugh^a, Kyle Gluesenkamp^b, Ahmad Abu-Heiba^b, Morteza Alipanah^a, Abdy Fazeli^a, Richard Rode^a, Michael Schmid^a, Viral Patel^b, Saeed Moghaddam^{a, *}

^a Department of Mechanical and Aerospace Engineering, University of Florida, Gainesville, FL 32603, USA

^b Building Equipment Research Group, Energy & Transportation Science Division, Oak Ridge National Laboratory, TN, USA

ARTICLE INFO

Keywords:

Ionic liquid
Absorption
Water heating
Dehumidification

ABSTRACT

While the use of energy efficient absorption heat pumps has been typically limited to the high capacity commercial and industrial applications, the use of a semi-open absorption heat pump for water heating has been demonstrated to be an energy efficient alternative for residential scale applications. A semi-open absorption system uses ambient water vapor as the refrigerant in the absorber where its heat of phase change is transferred to the process water, cooling the solution in the absorber. The solution is pumped to the desorber, where by adding heat, the water vapor is released from the solution and condensed in the condenser. The heat of phase change of water vapor is transferred to process water again in the condenser. This cycle when implemented with a membrane-based absorber in a plate and frame form of heat exchanger using ionic liquids can overcome the challenges related to the system architecture of conventional absorption heat pumps like the lower efficiency at small scale, crystallization/corrosion issues with the desiccants and the high cost of hermetically sealed components. The cycle COP for such a system was previously demonstrated by Chugh et al. for high humidity conditions. In this experimental study, design improvements were made that expand the system's applicability to more practical and standardized test conditions. With these improvements, the performance of the system was evaluated. The results presented in this study demonstrate the improved system's viability as a heat pump water heater conforming to standard water heater test conditions. Performance was measured at a cycle thermal COP of 1.2 with a hot water delivery water temperature of 56 °C and ambient air at 19 °C and 49% RH.

Nomenclature

CCHP	combined cooling heat and power
COP	coefficient of performance
EF	energy factor
GWP	global warming potential
HPWH	heat pump water heater
IL	ionic liquid

RI	refractive index
RH	relative humidity
SHX	solution heat exchanger
UEF	uniform energy factor
VCS	vapor compression system
\dot{m}	mass flow rate (kg/s)
T	temperature (°C)
T _{a,dpinlet}	inlet air dew point temperature(°C)

[☆] This manuscript has been authored by the University of Florida under Award Number DE-EE0006718 and UT-Battelle, LLC under Contract No. DE-AC05-00OR22725 with the U.S. Department of Energy. The United States Government retains and the publisher, by accepting the article for publication, acknowledges that the United States Government retains a non-exclusive, paid-up, irrevocable, world-wide license to publish or reproduce the published form of this manuscript, or allow others to do so, for United States Government purposes. The Department of Energy will provide public access to these results of federally sponsored research in accordance with the DOE Public Access Plan (<http://energy.gov/downloads/doe-public-access-plan>).

* Corresponding author.

Email address: saeedmog@ufl.edu (S. Moghaddam)

1. Introduction

With rising energy demand and the dependence on fossil fuels, the world is facing the unprecedented challenge of climate change and energy security [1]. Energy saving in buildings represents a major opportunity to limit the rise in demand, since energy consumption in buildings represents over one-third of the global and ~40% of the US energy consumption [2]. Forecasts suggest that the energy demand of the building sector will substantially rise due to growth in developing countries [3,4]. To slow this growth in energy consumption and its environmental impacts, one of the fundamental research objectives is to develop more energy efficient technologies.

Water heating is responsible for a significant portion of the energy demand in the US residential building sector, consuming ~2 Quads of primary energy at a cost of close to \$32 Billion. To reduce this energy demand, recent research efforts have focused on developing efficient heat pump systems [5–7], combined power cycles [8] or load management [9,10]. Historically, the implementation of environmentally friendly and energy efficient absorption heat pumps has primarily been limited to high capacity cooling, heating or CCHP applications. The development of residential scale absorption systems has recently been the focus of significant research [11–16]. Two key factors that limit expansion of absorption systems into small scale applications are the commonly used heat exchanger type and the working fluids used. First, the large absorption heat pump architecture uses shell and tube type heat exchangers, which are not economical for small scale applications. Second, the common working fluid pairs, LiBr-H₂O and LiCl-H₂O, are prone to crystallization, requiring the deployment of expensive and complex control mechanisms for stable and reliable system operation. In addition, the high corrosion rates associated with these working fluids require system pH management and the use of expensive metals. The recently proposed gas-fired semi-open membrane-based architecture (Fig. 1) offers an efficient and economically viable platform for a robust and compact absorption-based heat pump system for residential scale water heating applications with the potential to reduce the dehumidification energy consumption as well.

The semi-open architecture, as discussed in [17], showcases the potential of this new architecture compared to existing closed absorption systems. The open absorber configuration improves economics as it eliminates the need for a hermetically sealed metal design and fabrica-

tion. Instead, the absorber can be made from polymers and high-volume manufacturing techniques, such as thermal forming, can be deployed. Through analytical evaluations it was demonstrated that for heat pump applications, a semi-open architecture can achieve a COP comparable to that of closed systems and significantly enhance the operating window of the cycle with a minor performance penalty. Since this system utilizes the ambient water vapor as the refrigerant, there is no concern of a low temperature cut off as in conventional heat pumps due to the freezing of condensed water over the evaporator coils. The desorber-condenser part of the cycle is similar to a closed absorption heat pump system configuration, the only difference being that air is present. The presence of air may reduce the condensing potential and warrants larger surface areas and higher driving temperatures than closed systems to meet the required hot water outlet temperature.

In the open absorber, since the water vapor is absorbed from the air stream, the air stream is dehumidified. When the absorber is in a conditioned or semi-conditioned environment, the reduction in water vapor content will result in the lowering of the latent cooling load. The latent load for indoor applications is typically in the range of 20–40%, but in certain climate zones and applications it can be as high as 100% [18]. A typical installation location for an absorption heat pump water heater is the garage or basement of the home. Garage humidity ratios can approach that of outdoor air, which dependent on climate, can be significantly higher than the indoor humidity ratio. Additionally, parts of homes with poor ventilation, for example basements, can have very high humidity levels which warrant a dedicated dehumidifier installation (19% of homes have a dedicated dehumidifier installed in the basement). Thus, an absorption heat pump water heater could remove the need for a separate dehumidifier in a house to maintain the air humidity within the specified range per the ASHRAE standard. Further, the water vapor which is condensed in the condenser can be drained or utilized in either a direct or indirect evaporative cooling process. This additional advantage will further lower the cooling load for the residential cooling system.

The implementation of a new class of ionic liquid (IL-H₂O) working pairs applicable to absorption systems has attracted significant research in the last decade [19–27]. ILs are the new state of the art salts which can remain liquid at room temperature and have an affinity to the various refrigerants used in absorption systems like water, ammonia etc. Additionally, the properties (vapor pressure, viscosity, and other thermophysical properties) of these ILs are tuneable, thereby allowing configurable working pairs which can be optimized for various climate

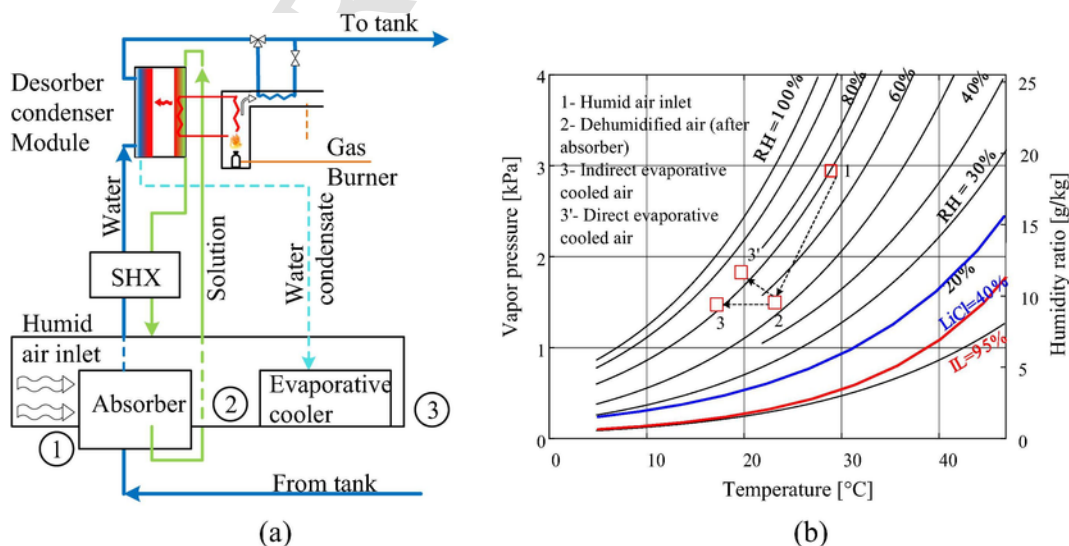


Fig. 1. (a) Process schematic of the semi-open absorption heat pump system. (b) Representative psychrometric processes for air flowing through the semi-open heat pump: state 3 is with indirect evaporative cooler, state 3' is with direct evaporative cooler.

conditions. The ILs can be heated to high temperatures (up to 200 °C) to meet the desired hot water outlet temperature. This is a major limitation in conventional absorption heat pumps where the highest temperature of the working pair is limited by crystallization and corrosion rates. Recently, Chugh et al. [5] experimentally demonstrated the use of ionic liquids for a residential scale heat pump water heating system and achieved cycle COP of almost 1.4. As outlined in [5], these ILs do not crystallize and have significantly lower corrosion rates eliminating the need for complex control mechanisms. However, the tests results discussed in [5] were done at favorable test conditions of high latent loads and with low water inlet temperatures. It was noted in that study that the system should be improved, specifically enhancement in the heat and mass transfer characteristics for the absorber and the desorber was required, to be able to test it at more practical and standardized test conditions.

In this study, a brief overview of the semi-open ionic liquid absorption-based HPWH system is presented. A description of the polymer absorber and the combined desorber-condenser module is presented, which enhances the performance of the semi-open absorption heat pump system and allows the testing of the heat pump water heater using ILs at standardized test conditions. Then the experimental system including all necessary auxiliary systems are described in detail. The system was evaluated under realistic/standardized water heating conditions and the results are presented and discussed.

2. System operation

The water heater system operation is described in detail in [5]. The system schematic and a very brief overview is presented here (Fig. 1A). The absorbent solution flowing through the absorber interfaces with

ambient water vapor through the membrane. The water vapor is then absorbed and its heat of phase change is released in the solution. The process water flowing through the absorber is heated by the hot absorbent solution. The water-laden solution is pumped to the desorber where it is heated by a heating fluid to release the absorbed water vapor. The process water flows from the absorber to a solution heat exchanger. The solution heat exchanger represents another novel feature of the cycle in that it permits the recovery of the heat energy from the solution exiting the desorber by heat exchange with process water rather than the conventional exchange with the solution exiting the absorber. The result is cooling of the solution prior to its entry into the absorber, and elevation of the process water temperature prior to its entry into the condenser. Upon entry into the condenser, the process water absorbs water vapor heat of phase change and exits the system. The condensed water is then either drained, if dehumidification is required, or it can be used in evaporative (direct or indirect) cooling. The state of the air flowing through the absorber-evaporator for the different possible operation configurations is shown in Fig. 1B.

3. Experimental test system

3.1. Test loop diagram

The absorption heat pump system was fabricated and coupled to a storage tank in an environmental chamber. Fig. 2 shows the schematic of the experimental set up. Two primary flow loops, namely solution (IL) and process water are circulated. The Uniform Plumbing Code (Section 602.1), as well as many locally enforced plumbing codes, prohibit connections where potable water could be contaminated with non-potable water either during normal operation or upon over-pres-

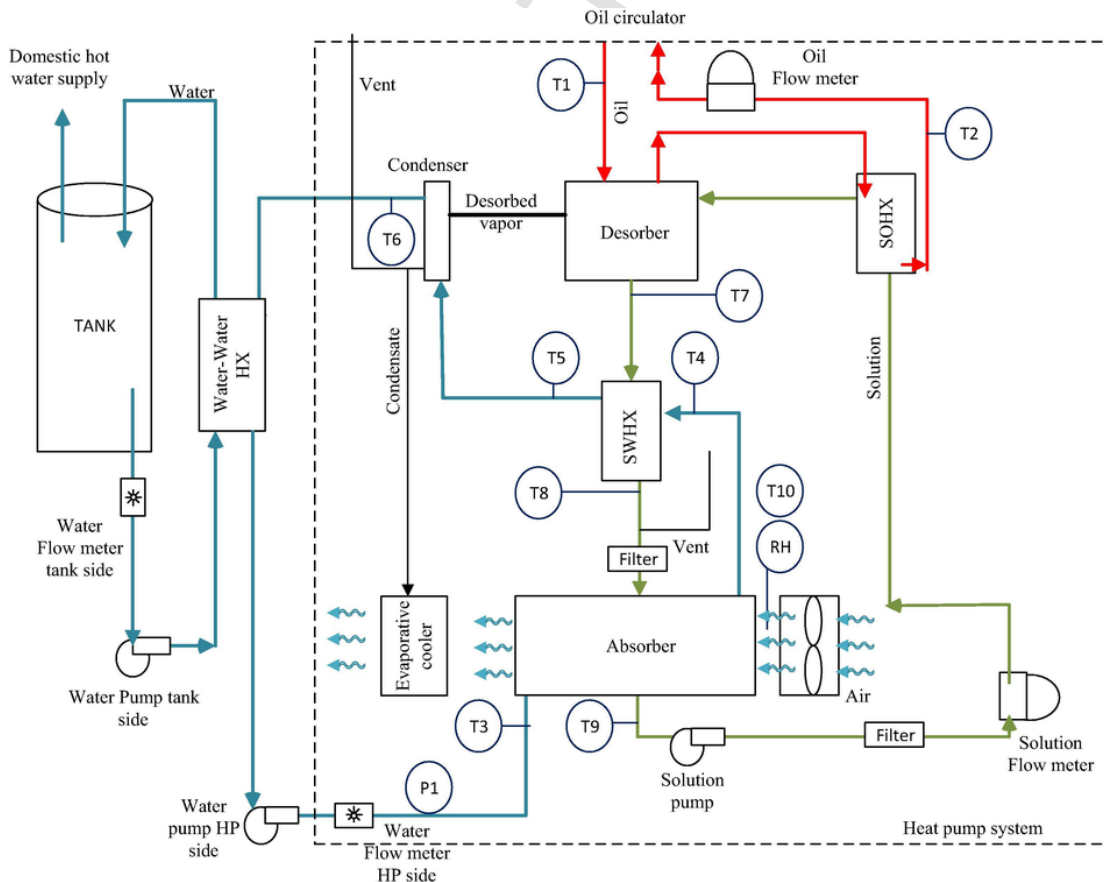


Fig. 2. Process and instrumentation diagram of the instrumented experimental test setup.

surizing part or the whole water supply system. Therefore, water from the storage tank could not be circulated through the heat pump and an intermediate plate-plate heat exchanger was used to transfer heat between the domestic water and the heat pump hot water stream. The inlet temperatures and flow rates of these fluid loops are measured and can be controlled independently. Additionally, two secondary fluid loops are required: the oil loop, which provides the heat input to the desorber, and a second heat transfer water loop which circulates water between the tank and the water-water heat exchanger. Fans are used to push the air through the absorber.

To maintain tank stratification in the hot water storage tank, the tank was heated by drawing the colder water from the bottom of the tank and returning the heated water to the top of the tank. The IL solution is pumped from the absorber exit to the desorber, exits the desorber and flows by gravity to the solution heat exchanger and then to the absorber. The process water to be heated enters the absorber, then flows to the solution heat exchanger and finally to the condenser.

3.2. Absorber

A schematic of the absorber is shown in Fig. 3. The absorber is fabricated from polycarbonate sheets. Two sheets of polycarbonate with machined channels for water flow are thermally bonded to form the internal channels for water flow. Post-thermal bonding features, as described in [5,12] are machined for the solution side structures. Following this, a chemical treatment of the polycarbonate surfaces is performed to make the surface hydrophilic. Then manifolds are bonded using adhesive and the membrane is bonded using a thermal bonding process. Air flows across the panels through a 3mm gap between membranes. The evaporator section is also installed right after the absorber section. However, the evaporative cooler part performance was not tested in this study as the focus was the heat pump section of the system.

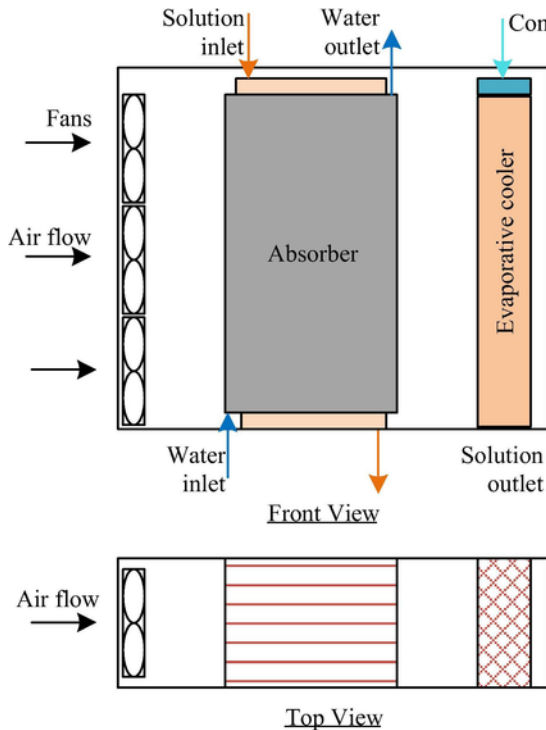


Fig. 3. Schematic of the absorber sub-assembly.

3.3. Desorber-Condenser module

The module design included an integrated desorbing and condensing surface as shown in Fig. 4, with a membrane separating the two. The membrane surface is superhydrophobic preventing its wetting by the solution. To enhance the desorption rate, the desorber used a structure similar to that used in the absorber, with a single two-sided brazed plate [11,28]. The two sides, desorbing and condensing, were bolted together with a gasketing material. The sub-assembly was leak tested with Nitrogen gas up to 5 PSI. Fig. 4 delineates the schematic and a picture of the fabricated desorber.

3.4. Heat exchangers

The two counter flow heat exchangers shown in Fig. 5 are used in the heat pump section. One transfers heat from solution to water, and the second from oil to solution. A third heat exchanger is used as heat exchange interface between the heat pump and the storage tank.

Instead of a gas burner, hot oil was used as the source of energy input to simulate fuel input. The temperature of the oil was controlled through a conditioning circulating bath. The circulator had an inte-

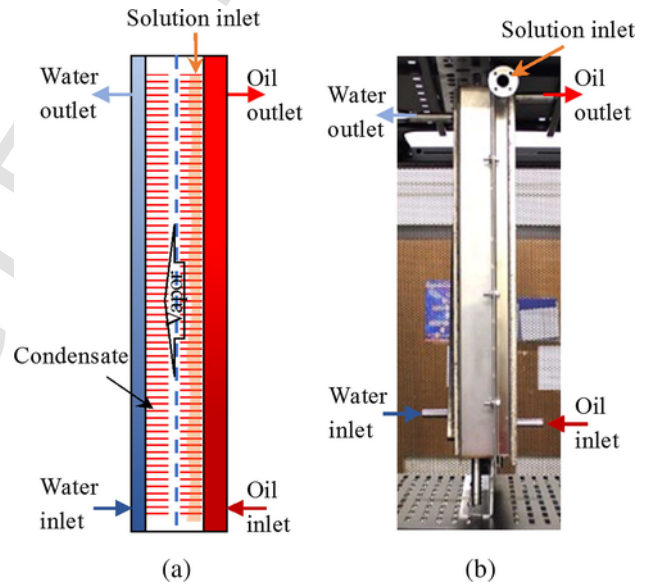


Fig. 4. (a) Schematic of the desorber-condenser module and (b) Photograph of the assembled desorber and condenser module.

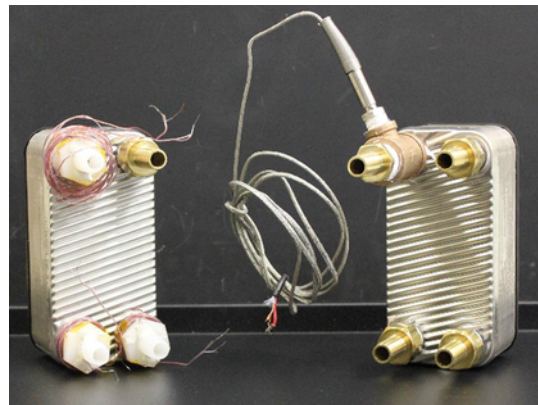


Fig. 5. Two heat exchangers used in the heat pump section with connections and thermocouples installed.

grated two-stage pump. The heat pump was integrated with a nominal 50-gallon storage tank. Domestic water was circulated via a variable speed pump to change flow rate as desired. City water was conditioned and circulated through a laboratory installed water conditioning supply system.

3.5. Measurement system

Oil, solution (IL) and process water flow rates were measured using Coriolis type mass flow meters. Domestic water volumetric flow rate was measured using an Alicat flow meter. All flow meters were calibrated in house using a bucket-stopwatch method. All temperatures were measured using T-Type thermocouples. Relative humidity measurements were made using Vaisala thin-film capacitive humidity sensors. Individual accuracies are listed in Table 1. Data was acquired from these sensors via a National Instruments cRIO data acquisition system on a one-second basis.

3.6. Data reduction and uncertainty analysis

The COP of the system is calculated using the Eq. (1)

$$COP = \frac{(Q_{absorber} + Q_{SHX} + Q_{Condenser})}{Q_{desorber}} \quad (1)$$

The uncertainty was calculated using an engineering equation solver (EES) subroutine for propagation of uncertainty. The subroutine is based on NIST guidelines [29] and assuming the individual measurements are uncorrelated and random, the uncertainty in the calculated quantity can be estimated as

$$U_Y = \sqrt{\sum_i \left[\frac{\partial Y}{\partial X_i} \right]^2 U_{X_i}^2} \quad (2)$$

Table 1 below lists all the relevant measurement errors and the uncertainties in this experimental study.

4. Results and discussion

4.1. Experimental testing

The objective of this study was to evaluate the steady state performance of the heat pump section of the system at the UEF and conditioned space conditions. Due to the solution heat loss that would occur through the addition of refractive index (RI) instruments in the test loop, the solution concentration is not measured in the present work. The lack of solution concentration measurements prevented conducting a full energy balance within the absorber and desorber/condenser module. However, energy balance based on RI measurements are reported in a previous study by authors [5]. Fig. 6 shows the system state points marked with steady state data on the components that were

Table 1
Measurement error and uncertainty propagation ORNL.

Variable	Uncertainty
Temperatures -All T-type TC	0.8 °C
Solution mass flow rate	± 1% reading
Process water mass flow rate	± 1% reading
Oil mass flow rate	± 0.5% reading
Air Relative humidity	± 1.5% RH
Water heat	± 2.0% (max value at UEF test condition)
COP	± 10.9% (max value at UEF test condition)

evaluated at the UEF condition. Fig. 7 demonstrates the temporal run at the UEF condition with water inlet and outlet temperatures and the total water heat transfer. Since this was an experimental test unit, manual control of valves to reach desired flow rates introduced certain limitations to achieve steady flow rates. Optimum fixed flow rate levels can be determined once more data is collected with future testing.

4.2. Comparison with previous generation heat pump (Chugh et al. 2017):

In a previous experimental study by Chugh et al. [5] a semi-open absorption heat pump was tested in a lab setting using the same IL. Table 2 below demonstrates the major differences between the absorber used in Chugh et al. (2017) and the absorber used in this study. The table shows a major increase in absorber area with lower envelope volume and improvement in the solution side and air solution interface. This permits more latent energy recovery per unit volume, which allows higher capacity systems with the same material and cost.

Fig. 8 compares the performance of the system evaluated in Chugh et al. [5] (at ambient air conditions of 30 °C, 70%RH) and this study (at different conditions). In Chugh et al. [5], the COP decreased with increasing capacity at a favorable test condition. The lower absorption rate of the absorber in Chugh et al. [5] had forced the testing to be done only at a favorable high latent load condition of 30 °C, 70%RH. Also, the inlet water temperature was maintained at 17.7 °C and it was noted that system performance decreased significantly at more practical air and water inlet temperature conditions. Enhancements in absorber area per unit volume and mass transfer characteristics were required to expand the system application to more real-world test conditions. In this study, some of the improvements are incorporated. Development of thin and light all polymer absorber panels and changing the manifolding system are among the improvements. Another key improvement is in the absorber mass transfer performance which was achieved through elimination of an air pocket formed between the process air and membrane in our previous design [5]. This improvement was accomplished through direct bonding of the membrane on polymer plates surface structures rather than using 3D printed polymer frames to hold the membrane. The system was tested at standardized UEF test conditions (19 °C, 49% RH), typical conditioned space conditions (21 °C, 51%RH), and humid conditions (25 °C, 74% RH) (the test matrix is listed in Table 3). The test conditions in the present study had less favorable air side conditions and less favorable supply water temperatures. Despite this, due to the higher surface area per unit volume and better absorber mass exchanger capacity as mentioned above, an equivalent or better COP was achieved. In addition, the system displayed a higher limit of incoming water temperature as is discussed in detail in the following sections.

4.3. COP and capacity

The COP of the system with the ambient dew point (DP) is shown in Fig. 9. Since the heat pump recovers the latent load from the ambient environment where it is installed, a higher latent load (higher DP) leads to a higher COP of the system. The heat pump involves a coupled heat and mass transfer phenomena in the absorber with three different fluids (air, absorbent and water) exchanging mass and thermal energy. The system performance at a given air dry bulb temperature (DBT) and relative humidity (RH) will not be the same at a different air DBT/RH value which may have an equivalent DP. Therefore, detailed system performance maps at relevant DBT/RH combinations to practical applications need to be developed. Performance of the system at some typical conditions that are of most practical significance have been evaluated and are reported in this study.

The COP and the capacity of the system is plotted against the water inlet temperature (T3 in Fig. 6) to the absorber in Figs. 10 and 11. Wa-

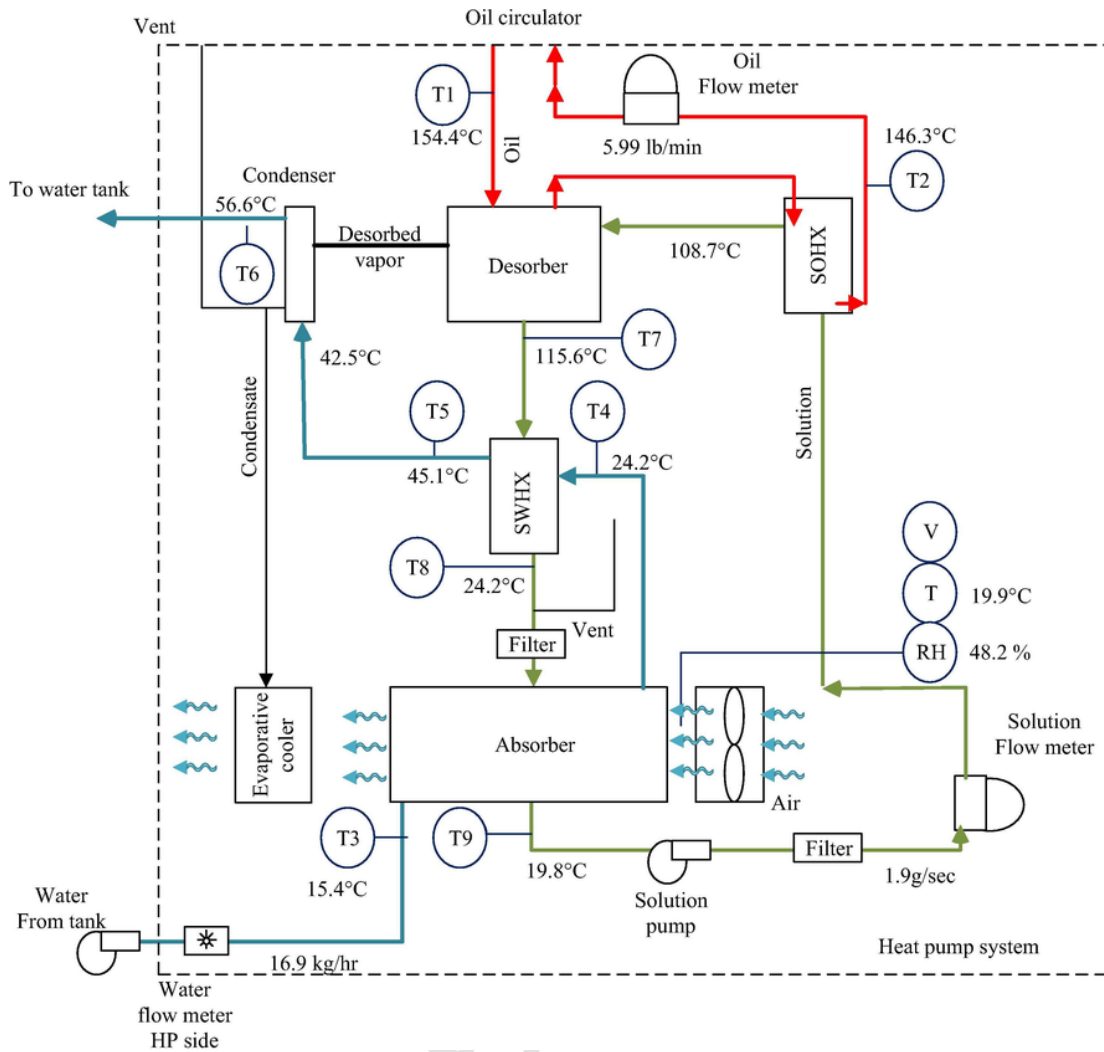


Fig. 6. This figure shows the evaluated components with the state point data at the steady state testing condition corresponding to UEF.

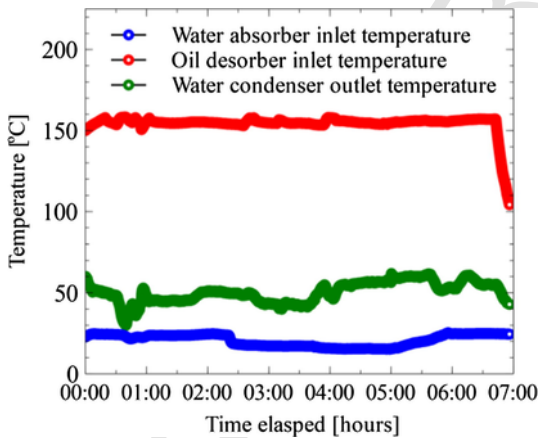


Fig. 7. Temporal run of the system demonstrating the startup, steady and shutdown condition.

ter inlet temperature is an important parameter as it affects the absorption potential of the absorbent in the absorber. The heat and mass transfer improvements in the absorber design in this study demonstrates that the system performance does not diminish beyond $T_{wi} > 30^\circ\text{C}$. This is a very important characteristic for heat pump water heaters as the inlet temperature of the water to the heat pump is

Table 2 Comparison of the absorber used in the Generation 1 and this study heat pump.

Absorber	Generation 1	This study
Number of panels	4	7
Active Surface area (m ²)	0.42	0.92
Active plate Volume (m ³)	0.0084	0.008
Active surface area/volume ratio	50	115
Material used	Water side: Metal (Cu/SS frame) Sol-water interface: SS sheet Fins: 1.5 mm tall made from Polymer (additive manufacturing)	All polymer (polycarbonate) Thermal and adhesive bonding, CNC machining used Fins: 1 mm tall
Membrane pore size	1 μm (commercially available) Not bonded on the fins	1 μm (same vendor as in Gen 1) Thermally bonded on fins

dependent upon several parameters, such as hot water load and water stratification in the tank. Achieving a minimal drop in the COP for high water temperature will allow the heat pump to operate at the required energy efficiency level for the full tank charge.

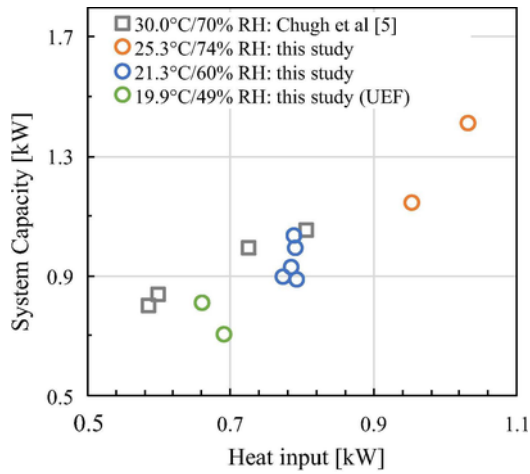


Fig. 8. Performance comparison of Chugh et al. (2017) to the current study: cycle COP with heat input.

Table 3

Test matrix for this study.

Ambient temperature/ relative humidity	Absorber inlet water temperature [°C]	Condenser outlet water temperature [°C]
21.3°C/60%	28.8	56.2
	23.0	50.9
	20.7	49.6
	18.0	48.8
	16.0	48.2
25.3°C/74%	17.3	61.3
	28.7	68.5
19.9°C/49%	15.4	56.6
	24.8	55.3

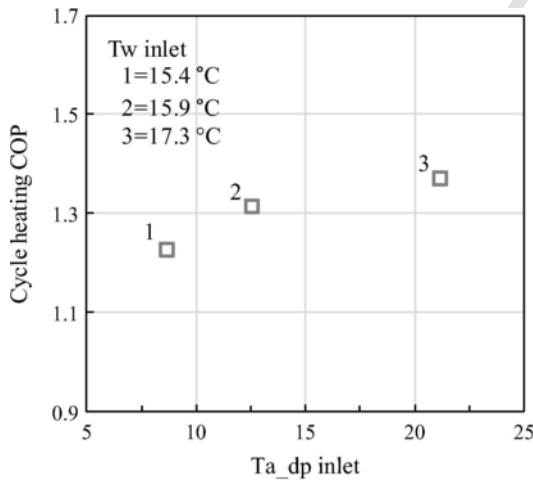


Fig. 9. COP as a function of air dew point.

The highest capacity and COP for the system are achieved for the highest DP condition of 25.3/74% RH. However, the relative lower performance of the system at the UEF condition could also be attributed to the higher heat losses from the whole system at a relatively cooler ambient condition.

It should be noted that the maximum recorded system capacity was 0.8kW at the standardized UEF test conditions, however the capacity of the system is a function of the number of absorber panels deployed

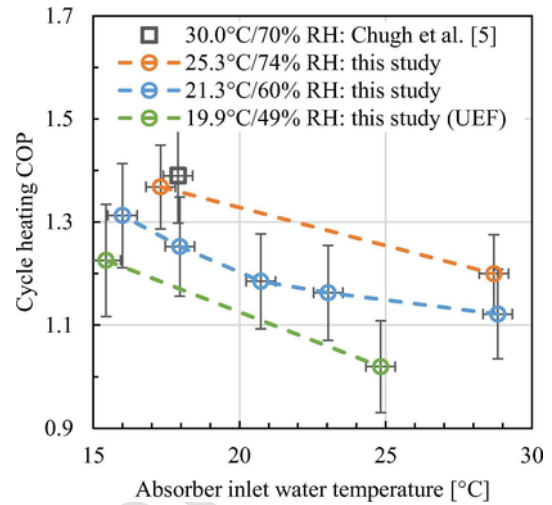


Fig. 10. COP of the heat pump as a function of water inlet temperature at different ambient conditions.

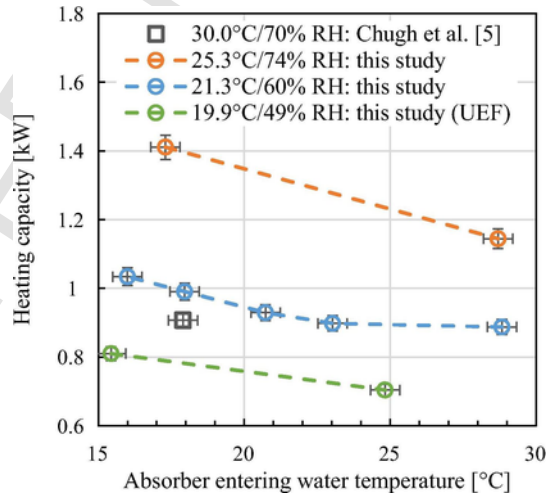


Fig. 11. Capacity of the heat pump as a function of water inlet temperature at different ambient conditions.

and the size of other system components (desorber/heat exchangers). A residential scale typical water heater heat pump will require a capacity of around 3kW (coupled with storage tank), therefore scaling the absorber (and other components) appropriately could potentially achieve a full-scale system for a residential scale application.

4.4. Hot water delivery temperature with water inlet temperature

Another important characteristic is the heat pump hot water outlet temperature. The residential water heating application has a requirement of about 55°C at the UEF condition as per the US Department of Energy standards. The hot water delivery temperature is shown in Fig. 12 and demonstrates that the heat pump evaluated in this study can deliver the water above the current requirement of the testing standard. It should be noted that while attempting to maintain a constant output hot water temperature (55°C), as required by the UEF condition (19.9°C ambient), the flow rate was manually adjusted. This imprecise change in water flow rate led to a relatively small decrease in the hot water delivery temperature. The water flow rate was not changed during the more favorable 25.3°C ambient air condition, leading to a higher delivery water temperature. A higher water flow rate was used during the 21.3°C trials, leading to generally lower heat pump delivery

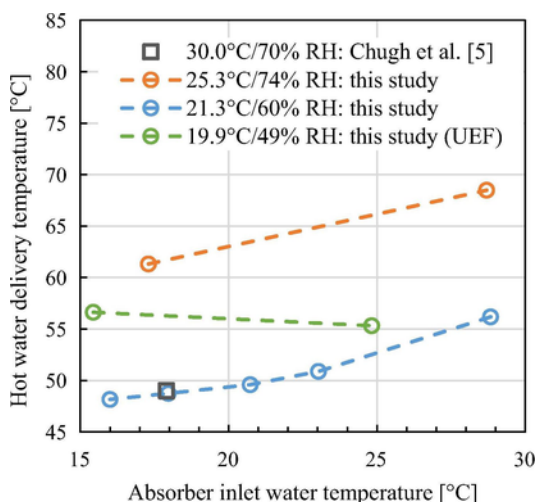


Fig. 12. Hot water delivery temperature as a function of absorber water inlet temperature at different ambient conditions.

temperatures. While the system meets the temperature requirement, adding more panels (surface area) provides the ability to achieve a higher system heating capacity.

5. Conclusion

Significant improvement has been made to a semi-open membrane-based absorption heat pump system for water heating application and the system has been tested in an environmental chamber at the Oak Ridge National Laboratory. The most important improvement is an all polymer-based absorber, the critical component of an absorption system which determines the efficacy of the system. The heat and mass exchanging improvement in the absorber is a $2 \times$ surface area to volume ratio increase with half the weight compared to the previous semi-open absorption system study. These enhancements allow the system to be tested at more practical test conditions like airconditioned space and standardized UEF test conditions. Additionally, these enhancements allow a higher water inlet temperature to the absorber for the water coming from the storage tank, thereby expanding the heat pump operation of the system for higher energy savings. The use of ionic liquids demonstrated the robustness of the system as there were no shutdowns related to corrosion and crystallization of the absorbent. At the standardized UEF test conditions the cycle COP obtained was 1.2 with a hot water discharge temperature of 56 °C. This efficiency is significant improvement over the existing gas fired storage tank water heaters.

Acknowledgments

This work was sponsored by the U. S. Department of Energy, Office of Energy Efficiency and Renewable Energy (EERE), under Award Number DE-EE0006718 with the University of Florida and DE-AC05-00OR22725 with UT-Battelle, LLC. The authors would also like to acknowledge Mr. Antonio Bouza, Technology Manager, Mr. Jim Payne, Technical Project Officer and Mr. Michael Geocaris, Project Engineer – HVAC&R, Water Heating, and Appliance, U.S. Department of Energy Building Technologies Office.

References

- [1] J. Yan, B. Chen, R. Wennersten, P. Campana, J. Yang, Cleaner energy for transition of cleaner city, *Appl Energy* 196 (2017) 97–99, <https://doi.org/10.1016/j.apenergy.2017.04.015>.

- [2] U.S. DOE. Quadrennial Technology Review: An Assessment of Energy Technologies and Research Opportunities, 2015. p. 1–505.
- [3] L.W. Davis, P.J. Gertler, Contribution of air conditioning adoption to future energy use under global warming, *Proc Natl Acad Sci* 112 (2015) 5962–5967, <https://doi.org/10.1073/pnas.1423558112>.
- [4] Å. Mi, Vuuren DP Van, Modeling global residential sector energy demand for heating and air conditioning in the context of climate change, *Energy Policy* 37 (2009) 507–521, <https://doi.org/10.1016/j.enpol.2008.09.051>.
- [5] D. Chugh, K. Gluesenkamp, O. Abdelaziz, S. Moghaddam, Ionic liquid-based hybrid absorption cycle for water heating, dehumidification, and cooling, *Appl Energy* 202 (2017) 746–754, <https://doi.org/10.1016/J.APENERGY.2017.05.161>.
- [6] J. Dong, Z. Zhang, Y. Yao, Y. Jiang, B. Lei, Experimental performance evaluation of a novel heat pump water heater assisted with shower drain water, *Appl Energy* 154 (2015) 842–850, <https://doi.org/10.1016/j.apenergy.2015.05.044>.
- [7] D. Zou, X. Ma, X. Liu, P. Zheng, B. Cai, J. Huang, et al., Experimental research of an air-source heat pump water heater using water-PCM for heat storage, *Appl Energy* 206 (2017) 784–792, <https://doi.org/10.1016/j.apenergy.2017.08.209>.
- [8] Y. Liang, M. Al-Tameemi, Z. Yu, Investigation of a gas-fuelled water heater based on combined power and heat pump cycles, *Appl Energy* 212 (2018) 1476–1488, <https://doi.org/10.1016/j.apenergy.2017.12.117>.
- [9] D. Sethaloo, S. Sichelalu, J. Zhang, Residential load management in an energy hub with heat pump water heater, *Appl Energy* 208 (2017) 551–560, <https://doi.org/10.1016/j.apenergy.2017.09.099>.
- [10] E.M. Wanjiru, S.M. Sichelalu, X. Xia, Model predictive control of heat pump water heater-instantaneous shower powered with integrated renewable-grid energy systems, *Appl Energy* 204 (2017) 1333–1346, <https://doi.org/10.1016/j.apenergy.2017.05.033>.
- [11] M. Mortazavi, R.N. Isfahani, S. Bigham, S. Moghaddam, Absorption characteristics of falling film LiBr (lithium bromide) solution over a finned structure, *Energy* 87 (2015) 270–278, <https://doi.org/10.1016/j.energy.2015.04.074>.
- [12] R. Nasr Isfahani, S. Bigham, M. Mortazavi, X. Wei, S. Moghaddam, Impact of micromixing on performance of a membrane-based absorber, *Energy* (2015) <https://doi.org/10.1016/j.energy.2015.08.006>.
- [13] M. Mortazavi, M. Schmid, S. Moghaddam, Compact and efficient generator for low grade solar and waste heat driven absorption systems, *Appl Energy* 198 (2017) 173–179, <https://doi.org/10.1016/j.apenergy.2017.04.054>.
- [14] G. Angrisani, M. Canelli, C. Roselli, A. Russo, M. Sasso, F. Turiello, A small scale polygeneration system based on compression/absorption heat pump, *Appl Therm Eng* 114 (2017) 1393–1402, <https://doi.org/10.1016/j.applthermaleng.2016.10.048>.
- [15] J. Aman, D.S.K. Ting, P. Henshaw, Residential solar air conditioning: Energy and exergy analyses of an ammonia-water absorption cooling system, *Appl Therm Eng* 62 (2014) 424–432, <https://doi.org/10.1016/j.applthermaleng.2013.10.006>.
- [16] A. Ondeck, T.F. Edgar, M. Baldea, A multi-scale framework for simultaneous optimization of the design and operating strategy of residential CHP systems, *Appl Energy* 205 (2017) 1495–1511, <https://doi.org/10.1016/j.apenergy.2017.08.082>.
- [17] K.R. Gluesenkamp, D. Chugh, O. Abdelaziz, S. Moghaddam, Efficiency analysis of semi-open sorption heat pump systems, *Renew Energy* (2016) 1–10, <https://doi.org/10.1016/j.renene.2016.07.075>.
- [18] Kozubal E, Woods J, Burch J, Boranian A, Merrigan T. Desiccant Enhanced Evaporative Air-Conditioning (DEVap): evaluation of a new concept in ultra efficient air conditioning; 2011.
- [19] P. Chatzitakis, B. Dawoud, An alternative approach towards absorption heat pump working pair screening, *Renew Energy* (2016) <https://doi.org/10.1016/j.renene.2016.08.014>.
- [20] I. Sujatha, G. Venkatarathnam, Performance d'un système frigorifique à absorption de vapeur opérant avec des hydrofluorocarbures et des hydrofluorooléfines comme frigorigènes et du liquide ionique [hmim][TF2N] comme absorbant, *Int J Refrig* 88 (2018) 370–382, <https://doi.org/10.1016/j.ijrefrig.2018.03.004>.
- [21] M. Mortazavi, S. Moghaddam, Laplace transform solution of conjugate heat and mass transfer in falling film absorption process Solution de la transform{é}e de Laplace du transfert de chaleur et de masse conjugu{é} dans un processus d'absorption à film tombant, *Int J Refrig* 66 (2016) 93–104, <https://doi.org/10.1016/j.ijrefrig.2016.02.013>.
- [22] Y.J. Kim, S. Kim, Y.K. Joshi, A.G. Fedorov, P.A. Kohl, Thermodynamic analysis of an absorption refrigeration system with ionic-liquid/refrigerant mixture as a working fluid, *Energy* 44 (2012) 1005–1016, <https://doi.org/10.1016/j.energy.2012.04.048>.
- [23] A. Giampieri, Z. Ma, A. Smallbone, A.P. Roskilly, Thermodynamics and economics of liquid desiccants for heating, ventilation and air-conditioning – An overview, *Appl Energy* 220 (2018) 455–479, <https://doi.org/10.1016/j.apenergy.2018.03.112>.
- [24] A. Cera-Manjarres, D. Salavera, A. Coronas, Vapour pressure measurements of ammonia/ionic liquids mixtures as suitable alternative working fluids for absorption refrigeration technology, *Fluid Phase Equilib* (2018) <https://doi.org/10.1016/j.fluid.2018.01.006>.
- [25] D. Moreno, V.R. Ferro, J. de Riva, R. Santiago, C. Moya, M. Larriba, et al., Absorption refrigeration cycles based on ionic liquids: Refrigerant/absorbent selection by thermodynamic and process analysis, *Appl Energy* 213 (2018) 179–194, <https://doi.org/10.1016/j.apenergy.2018.01.034>.
- [26] S. Kim, P.A. Kohl, Analysis of [hmim][PF6] and [hmim][TF2N] ionic liquids as absorbents for an absorption refrigeration system, *Int J Refrig* 48 (2014) 105–113, <https://doi.org/10.1016/j.ijrefrig.2014.09.003>.

- [27] Schneider MC, Schneider R, Zehnacker O, Buchin O, Cudok F, Kühn A, et al. Ionic Liquids: New high-performance working fluids for absorption chillers and heat pumps. In: Proc Int Sorption Heat Pump Conf, vol. 6; 2011.
- [28] S. Bigham, R. Nasr Isfahani, S. Moghaddam, Direct molecular diffusion and micro-mixing for rapid dewatering of LiBr solution, Appl Therm Eng 64 (2014) 371–375, <https://doi.org/10.1016/j.applthermaleng.2013.12.031>.
- [29] B.N. Taylor, C.E. Kuyatt, Guidelines for evaluating and expressing the uncertainty of NIST measurement results, Technology 2 (1994).

UNCORRECTED PROOF